THE JOURNAL OF BIOLOGICAL CHEMISTRY
Vol. 278, No. 47, Issue of November 21, pp. 46938–46948, 2003
Printed in U.S.A.

Thermodynamic Description of the Effect of the Mutation Y49F on Human Glutathione Transferase P1-1 in Binding with Glutathione and the Inhibitor *S*-Hexylglutathione*

Received for publication, May 14, 2003, and in revised form, August 7, 2003
Published, JBC Papers in Press, August 23, 2003, DOI 10.1074/jbc.M305043200

Emilia Ortiz-Salmerón‡, Marzia Nuccetelli§, Aaron J. Oakley¶‖, Michael W. Parker¶, Mario Lo Bello§**‡‡, and Luis García-Fuentes‡**§§**

From the ‡Physical Chemistry, Faculty of Experimental Sciences, University of Almería, La Cañada de San Urbano, Almería 04120, Spain, the §Children's Hospital IRCCS "Bambino Gesù" 00165, Rome, Italy, ¶Biota Structural Biology Laboratory, St. Vincent's Institute of Medical Research, Fitzroy, Victoria 3065, Australia, and the ‡‡Department of Biology, University of Rome "Tor Vergata," Via della Ricerca Scientifica, Rome 00133, Italy

The thermodynamics of binding of both the substrate glutathione (GSH) and the competitive inhibitor *S*-hexylglutathione to the mutant Y49F of human glutathione *S*-transferase (hGST P1-1), a key residue at the dimer interface, has been investigated by isothermal titration calorimetry and fluorescence spectroscopy. Calorimetric measurements indicated that the binding of these ligands to both the Y49F mutant and wild-type enzyme is enthalpically favorable and entropically unfavorable over the temperature range studied. The affinity of these ligands for the Y49F mutant is lower than those for the wild-type enzyme due mainly to an entropy change. Therefore, the thermodynamic effect of this mutation is to decrease the entropy loss due to binding. Calorimetric titrations in several buffers with different ionization heat amounts indicate a release of protons when the mutant binds GSH, whereas protons are taken up in binding *S*-hexylglutathione at pH 6.5. This suggests that the thiol group of GSH releases protons to buffer media during binding and a group with low pK_a (such as Asp^{98}) is responsible for the uptake of protons. The temperature dependence of the free energy of binding, ΔG^0, is weak because of the enthalpy-entropy compensation caused by a large heat capacity change. The heat capacity change is -199.5 ± 26.9 cal K^{-1} mol^{-1} for GSH binding and -333.6 ± 28.8 cal K^{-1} mol^{-1} for *S*-hexylglutathione binding. The thermodynamic parameters are consistent with the mutation Tyr^{49} → Phe, producing a slight conformational change in the active site.

Molecular recognition phenomena are at the heart of biological reactions. A key to understanding molecular recognition is a comprehensive analysis of the thermodynamics of binding and the meaningful correlation of thermodynamics with the structure. A close insight into the thermodynamics of the binding process provides guide marks for structure-based molecular design strategies. The forces that govern a binding reaction are the free energy change, ΔG, the enthalpy change, ΔH, the entropy change, ΔS, and the heat capacity change, ΔC_p. ΔC_p is an approximate measure of the surface area buried in an association reaction and can be used to predict conformational rearrangements in associating protein molecules. An example of particular medical interest is human glutathione transferase P1-1 (hGST P1-1). The structure of this enzyme is known at high resolution in complex with a series of ligands, including its substrate glutathione (GSH) and numerous inhibitors (1–3).

Glutathione *S*-transferases (GSTs[1]; EC 2.5.1.18) are a family of dimeric detoxification enzymes that catalyze the conjugation of GSH to a variety of endogenous and exogenous electrophiles. The mammalian cytosolic GSTs have been grouped into at least seven species-independent classes based on crystal structure and substrate specificity: Alpha, Pi, Mu, Theta, Kappa, Sigma, and Zeta (4–8). Comparison of the primary structures among the different classes reveals a very low degree of sequence identity (~25%). However, crystal structures of GSTs display a common three-dimensional fold and a dimeric organization. All of the cytosolic isozymes are either homo- or heterodimers, whereas no interclass heterodimers have so far been observed (9). Each monomer comprises two domains with one active site. The main structural differences among GST classes are in the GSH binding site (G-site) (in particular, the helix α_2 region) and in the hydrophobic substrate binding site (H-site). The human Pi class GST (hGST P1-1) is the most widely distributed and the most abundant of the isoenzymes. Some studies have implicated this enzyme in the development and resistance of tumors toward commonly used anticancer drugs. Understanding the structure and kinetics of the human P1-1 isoenzyme is therefore of great interest (9). Kinetic studies have revealed the importance of the helix α_2 in the function of the enzyme (10, 11). The crystal structures suggest that helix α_2 and its flanking regions (residues 35–51) are a prime candidate for the flexible regions that are known to influence catalysis. A number of residues of from this region (Trp^{38}, Lys^{44}, and Gln^{51}) participate in the binding of GSH (Fig. 1). Other studies indicate that several residues, such as Cys^{47} and Tyr^{49}, which are

* This work was supported in part by DGICYT Team SAF2001-2067; Ministerio de Ciencia y Tecnología (Spain), Plan Andaluz de Investigación Team CVI-900; MIUR, Ministero dell'Istruzione, Università e Ricerca, COFIN 2002; an Australian Research Council Project Team; a National Health and Medical Research Council (NHMRC) of Australia Senior Principal Research Fellowship (to M. W. P.); and a NHMRC Postgraduate Research Scholarship (to A. J. O.). The costs of publication of this article were defrayed in part by the payment of page charges. This article must therefore be hereby marked "*advertisement*" in accordance with 18 U.S.C. Section 1734 solely to indicate this fact.

‖ Present address: A. J. Oakley, Dept. of Pharmacology, The Queen Elizabeth II Medical Centre, Nedlands, Western Australia 6009, Australia.

** These three authors are senior co-authors.

§§ To whom correspondence should be addressed. Tel.: 34-950-015618; Fax: 34-950-015008; E-mail: lgarcia@ual.es.

[1] The abbreviations used are: GST, glutathione *S*-transferase; hGST, human GST; *S*-hexylGSH, *S*-hexylglutathione; ITC, isothermal titration calorimetry; MES, 2-(*N*-morpholino)ethanesulfonic acid; MOPS, 3-(*N*-morpholino)propanesulfonic acid; ACES, 2-[(2-amino-2-oxoethyl)-amino]ethanesulfonic acid; DTT, dithiothreitol.

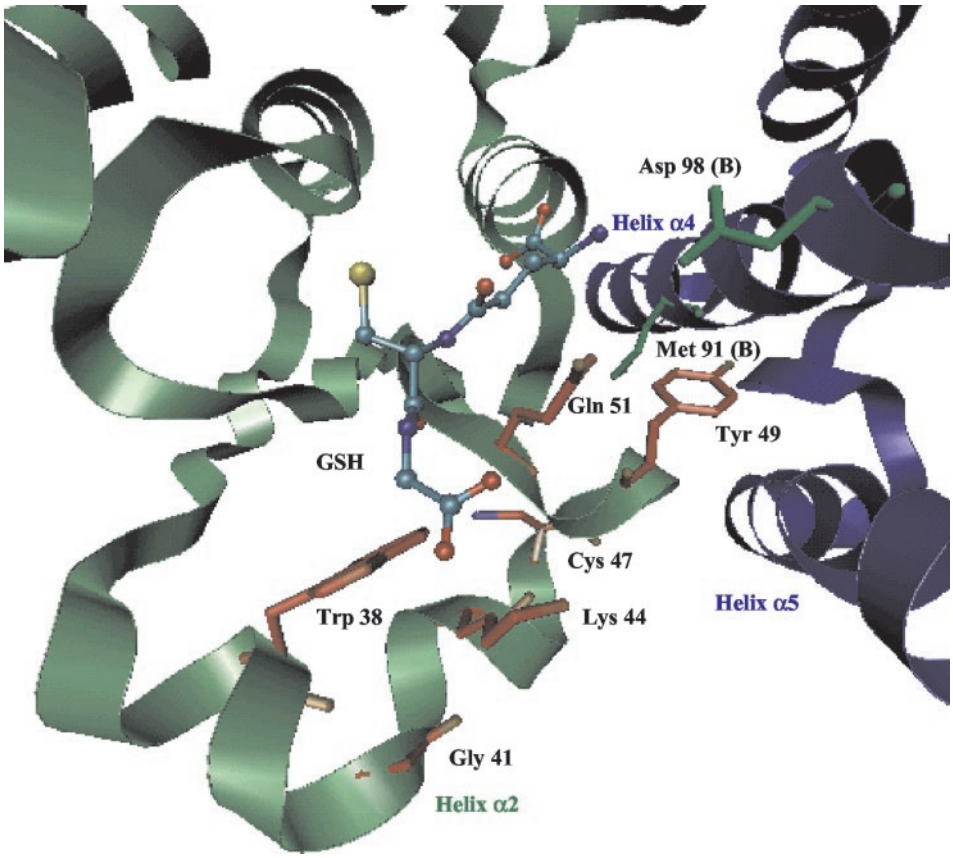

FIG. 1. **Schematic representation of the binding site of GSH (G-site) in homodimeric hGST P1-1.** Subunits are displayed in *green* and *blue*. The GSH molecule is shown in a *ball-and-stick* representation. Helix α_2 is denoted, and residues from this helix and its flanking region that directly contact GSH are also shown. Some residues of the adjacent subunit that also participate in the active site are indicated. This *figure* was made using VMD software (49) and corresponds to entry 7GSS of the Protein Data Bank (3).

located between helices α_4 and α_5 of the adjacent subunit (Fig. 1), could participate in intersubunit communication between active sites of the dimer (1, 12). Although some studies have already been performed with the mutant Y49F in the presence of co-substrate (13), there has been no thermodynamic study carried out on this mutant in the absence of the co-substrate.

We have initiated a study of each of these residues with the aim of understanding their relative roles in substrate binding of hGST P1-1. In this paper, we have focused our study on the binding of GSH and the inhibitor *S*-hexylglutathione (*S*-hexyl-GSH) to the Y49F mutant of hGST P1-1 using fluorescence spectroscopy and isothermal titration microcalorimetry (ITC). The results are compared with those obtained for the wild-type enzyme and discussed in terms of possible differences in their interaction with ligands.

EXPERIMENTAL PROCEDURES

Chemicals—GSH, S-hexylGSH, and 1-chloro-2,4-dinitrobenzene were ultrapure grade from Sigma. Dithiothreitol (DTT) was from Amersham Biosciences. Phosphate, MOPS, MES, and ACES buffers were purchased from Merck and Sigma. All other chemicals were of analytical grade of the highest purity available. All solutions were made with distilled and deionized (Milli Q) water. All solutions were degassed and filtered through a 0.45-μm Millipore filter before use.

Protein Expression and Purification—The wild-type hGST P1-1 was obtained as previously reported (14). The Y49F mutant was designed and produced by site-directed mutagenesis, carried out in a two-step polymerase chain reaction (15). Details of this procedure have been reported elsewhere (13). Finally, the Y49F mutant was expressed in TOP 10 *Escherichia coli* cells and purified as previously reported (14).

Estimation of Protein Concentration—Solutions of wild-type and Y49F mutant were prepared by dialysis of the enzyme against several changes of buffer solution at 4 °C. Protein concentrations were determined from absorbance measurements at 280 nm using an extinction coefficient of $5.44 \cdot 10^4$ $M^{-1} \cdot cm^{-1}$ for the dimer. The extinction coefficient was calculated on the basis of the amino acid sequence as reported by Gill *et al.* (16) and confirmed by the bicinchoninic acid method (Pierce). Absorbance measurements were carried out using a Beckman DU-7400 spectrophotometer with cells maintained at 25 °C.

Crystallization—Crystallization was performed by the hanging drop vapor diffusion method as described elsewhere (3). Briefly, a 2-μl drop of a protein solution containing Y49F in 1 mM EDTA, 1 mM mercaptoethanol, and 10 mM phosphate buffer (pH 7.0) was mixed with an equal volume of reservoir solution, which consisted of 25% (w/v) ammonium sulfate, 60 mM DTT, and 100 mM MES buffer (pH 5.8). The trials were carried out at a constant temperature of 22 °C. The drops were allowed to equilibrate for 1 day before they were streak-seeded with a cat's whisker from drops containing wild-type crystals grown under similar conditions. Crystals appeared in the shape of plates after 1 week and grew to maximal dimensions of 0.1 × 0.3 × 0.3 mm. The x-ray diffraction data were collected using a MARResearch area detector with Cu$K\alpha$ X-rays generated by a Rigaku RU-200 rotating anode x-ray generator. The data were collected at 100 K after cryoprotecting the crystals in 25% (v/v) glycerol. The diffraction data were processed and analyzed using programs in the HKL (17) and CCP4 (18) suites. The data collection statistics are presented in Table I.

Structure Determination—Refinement began with the Pi class GST in the C2 space group (5GSS) (3), which had GSH and water molecules removed. Rigid body refinement in XPLOR (19) was used to compensate for any possible changes in crystal packing. Since the asymmetric unit of the crystal contained two GST monomers, use was made of the noncrystallographic symmetry restraints on all non-hydrogen atoms during the first few rounds of refinement. The starting model gave an *R*-factor of 34.0% (R_{free} = 34.3%), which reduced to 32.5% (R_{free} = 32.3%) after rigid body refinement. The mutation was clearly observed in an $F_{mutant} - F_{wild\ type}$ electron density map with −5 σ peaks over the hydroxyl groups of Tyr^{49} in each monomer, and hence residue 49 was changed to phenylalanine. The model was then subjected to cycles of positional and isotropically restrained B-factor refinement and inclusion of water and buffer molecules. After application of a bulk solvent

TABLE I
Data Collection and Processing for Y49F

Temperature (K)	100
Space group	C2
Cell dimensions	
a (Å)	77.8
b (Å)	90.0
c (Å)	68.9
β (degrees)	97.9
Maximum resolution (Å)	1.9
No. of crystals	1
No. of observations	94,042
No. of unique reflections	35,081
Data completeness (%)	95.0(92.2)[a]
Completeness $> 3\sigma_I$ (%)	79.7(57.1)[a]
I/σ_I	16.2(5.6)[a]
Multiplicity	2.7
R_{merge}[b] (%)	6.0(18.0)

[a] The values in parentheses are for the highest resolution bin (approximate interval of 0.05 Å).
[b] $R_{merge} = \Sigma_{hkl}\Sigma_i|I_i - \langle I\rangle|/|\langle I\rangle|$, where I_i is the intensity for the *i*th measurement of an equivalent reflection with indices *h*,*k*,*l*.

TABLE II
Refinement statistics for Y49F

Non-hydrogen atoms	
Protein	3260
Substrate/inhibitor	0
MES	36
Solvent	312
Resolution (Å)	1.9
$R_{conv.}$ (%)	20.6
R_{free} (%)	23.0
Reflections used in $R_{conv.}$ calculations	
Number	33,336
Completeness (%)	89.9
Root mean square deviations from ideal geometry	
Bonds (Å)	0.007
Angles (degrees)	1.3
Dihedrals (degrees)	23.1
Impropers (degrees)	0.74
Bonded Bs (Å^2)	2.6
Mean B (protein) (Å^2)	
Main chain	14.1
Side chain	17.0
Mean B (solvent) (Å^2)	24.3
Residues in most favored regions of Ramachandran plot (%)	94.1

correction, the final *R*-factor was 20.6% (R_{free} = 23.0%) for all data to 1.9-Å resolution. A stereochemical analysis of the refined structure with the program PROCHECK (20) gave values either similar to or better than expected for structures refined at similar resolution. The final refinement statistics are presented in Table II.

Fluorescence Measurements—The binding of GSH and *S*-hexylglutathione to the Y49F mutant of hGST P1-1 was followed by intrinsic fluorescence quenching of the enzyme after ligand addition, using a PerkinElmer LS50B spectrofluorometer interfaced to a computer for data collection. The excitation wavelength was 278 nm, and fluorescence was monitored at 339 nm. The temperature of the sample was controlled at 25.0 ± 0.2 °C using a thermostatted cuvette holder and a Frigiterm 6000382 Selecta refrigerated circulating water bath. A 2.0-ml protein solution in a 4.0-ml quartz fluorescence cell was stirred after each addition of ligand. The emission slit widths used for excitation and emission were 4 nm. The buffer used for fluorescence was 50 mM sodium phosphate, 5 mM NaCl, 0.1 mM EDTA, and 1 mM DTT at pH 6.5. The fluorescence measurements were corrected for dilution and inner filter effects. The procedure and data analysis used were similar to that described elsewhere (21).

Isothermal Titration Microcalorimetry—ITC experiments were carried out using an MCS titration microcalorimeter (Microcal Inc., Northampton, MA) (22). The reference cell was filled with Milli Q water, and the calorimeter was calibrated using standard electrical pulses, as recommended by the manufacturer. Prior to the titration experiments, both enzyme and ligand were degassed for 10 min under vacuum. Solutions of the proteins were filled in the sample cell (1.38-ml volume) and titrated with either GSH or *S*-hexylGSH. Ligand solutions were prepared in the buffer from the last change of dialysis. During the titration, the reaction mixture was continuously stirred at 400 rpm. A typical experiment consisted of a first control injection of 1 or 2 μl followed by successive injections, each of 5 μl of 20-s duration, with a 4-min interval between injections. The background titration profiles, under identical experimental conditions, were obtained by injecting the ligand into appropriate buffer solutions. The observed heat effects were concentration-independent and were identical to the heat signals detected after complete saturation of the protein. The raw experimental data was presented as the amount of heat produced per second following each injection of ligand into the enzyme solution (corrected for the ligand heats of dilution) as a function of time. The amount of heat produced per injection was calculated by integration of the area under individual peaks by the Origin software provided with the instrument.

ITC measurements were routinely performed in 5 mM NaCl, 0.1 mM EDTA, 1 mM DTT, and 50 mM of sodium phosphate at pH 6.5. Heat contributions due to coupled protonation events upon binding were evaluated by calorimetric experiments in various buffers, and their ionization enthalpies (in kcal mol^{-1} at 25 °C) were as follows: phosphate (1.22), MES (3.72), MOPS (5.27), and ACES (7.53) (23). The pH of the buffer solutions was adjusted at the experimental temperature.

RESULTS

Fluorescence Binding Experiments

The binding of *S*-hexylGSH and the GSH to the Y49F mutant of hGST P1-1 was observed by intrinsic fluorescence as a function of the ligand concentration at 25 °C and pH 6.5, following the procedure indicated under "Experimental Procedures." Fig. 2 depicts the titrations of this mutant with these ligands (*i.e.* GSH (*A*) and *S*-hexylGSH (*B*)). The titrations were displayed as a plot of the degree of binding, ν, *versus* log[ligand], with [ligand] being the ligand free concentration (GSH or *S*-hexylGSH). Extrapolation of the upper part of the plots leads to a value of 2 mol of ligand bound per mol of dimeric enzyme at saturation. A Scatchard plot of these values clearly extrapolates to ν = 2 (plots shown as an *inset* in Fig. 2), and no systematic deviations from linearity are detected. These results may be taken as evidence of the existence of two identical and independent binding sites. A Hill plot of these experimental values leads to Hill coefficients of 0.96 ± 0.06 and 0.98 ± 0.03 for the binding of GSH and *S*-hexylGSH, respectively, indicating that the binding of these ligands to Y49F mutant is noncooperative. The fitting of these experimental data to this model gives a value for the association constant, *K*, of (4.8 ± 0.3) × 10^3 M^{-1} (K_d = 205 μM) and (2.7 ± 0.6) × 10^5 M^{-1} (K_d = 3.7 μM) for the binding of GSH and *S*-hexylGSH, respectively. These values are ~3-fold and 6-fold lower than those obtained for the wild-type enzyme: 7.7 × 10^3 M^{-1} (K_d = 130 μM) (13) and (7.8 ± 0.5) × 10^5 M^{-1} (K_d = 1.27 μM) for GSH and *S*-hexylGSH binding, respectively.

ITC Experiments

Direct calorimetric measurements were performed in order to obtain independent estimates of the thermodynamic parameters governing binding of GSH and *S*-hexylGSH to the Y49F mutant and the wild-type enzyme. Figs. 3 and 4 show representative titrations of the Y49F mutant with GSH and *S*-hexylGSH, respectively. Representative titrations of wild-type with both ligands appear also as an *inset* plot in Figs. 3 and 4. The enthalpy change ΔH and binding constant *K* on enzyme-ligand interaction were directly obtainable from the experimental titration curves shown in Figs. 3 and 4. Moreover, the Gibbs energy change of binding ($\Delta G = -RT\ln K$) was calculated from the binding constant, and the entropy change ($T\Delta S = -\Delta G + \Delta H$) on the association was also estimated.

Change of Protonation State—Substrate or inhibitor binding may cause the enzyme to take up or release protons (*e.g.* through pK_a changes of the side chains accompanying the binding reaction). This will contribute to the overall heat change, ΔH_{obs}, measured in the ITC experiment. If ionizable

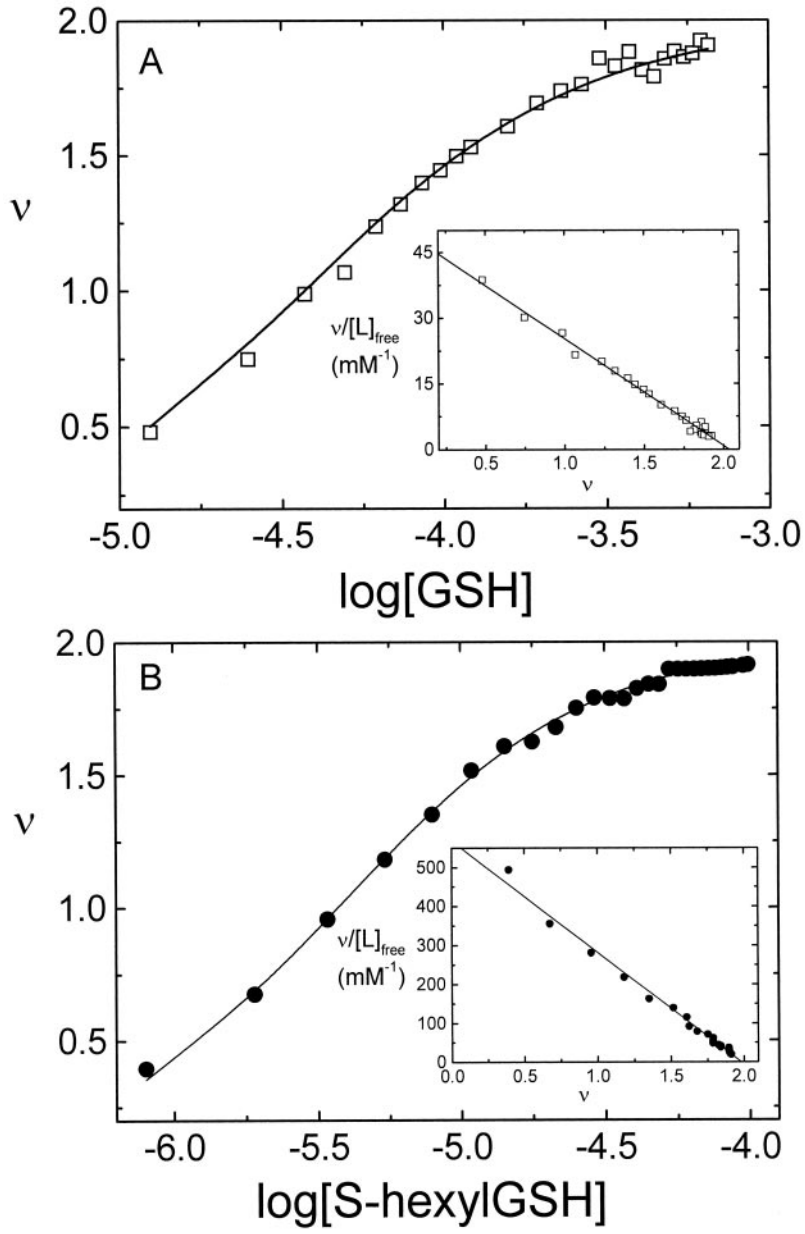

FIG. 2. **Binding of GSH (*A*) and *S*-hexylGSH (*B*) to Y49F mutant of hGST P1-1 obtained by fluorescence spectroscopy at pH 6.5 and 25 °C.** The degree of binding, ν, is plotted *versus* log [ligand]. The dimeric enzyme concentrations were 8.32 μM (GSH binding) and 9.73 μM (*S*-hexylGSH binding), and the buffer solution was 50 mM sodium phosphate, 5 mM NaCl, 0.1 mM EDTA, and 1 mM DTT. The *solid line* gives the best fit to the data for a noncooperative model. The plots displayed as *inset* in both *panels* represent the Scatchard plots for these associations.

groups undergo pK_a changes on complex formation, protons will be exchanged with the buffer. The heat of protonation/deprotonation depends on the ionization enthalpy of the buffer to the following equation,

$$\Delta H_{obs} = \Delta H_{bind} + n_{H^+}\Delta H_{ioniz} \quad \text{(Eq. 1)}$$

where n_{H^+} designates the number of protons that are taken up ($n_{H^+} > 0$) or released ($n_{H^+} < 0$) by the complex protein-ligand (24). To study such protonation effects, calorimetric titration experiments were repeated in various buffers of different ΔH_{ioniz} (MOPS, MES, ACES, and phosphate) at pH 6.5 and 25 °C. The binding enthalpy, ΔH_{bind}, was obtained from the intercept ($\Delta H_{ioniz} = 0$) of a plot according to Equation 1. The results are shown in Table III and Fig. 5. A negative slope was obtained ($n_{H^+} < 0$), with $n_{H^+} = -0.44 \pm 0.08$ and $n_{H^+} = -0.11 \pm 0.01$ for the binding of GSH to the wild type and the Y49F mutant, respectively (Table III). Hence, in the complex formation enzyme-GSH, the number of protons released for wild-type enzyme is higher than that for the Y49F mutant. This means that one or several pK_a values, corresponding to some donor proton groups of the ligand and/or enzyme, decrease (*i.e.* become more acidic). Since ~0.45 H^+/monomer are released in the wild-type/GSH binding, few groups will be able to change their pK_a value. In fact, a common feature of GSTs, which have very similar GSH binding sites (G-sites), is that they lower the apparent pK_a value of the bound GSH from 9.1 to about 6.0–6.6. The hydroxyl group of a conserved tyrosine or serine (for instance, Tyr^7 in this transferase; Tyr^9 in the Alpha class GST A1–1; Tyr^6 in *Schistosoma japonicum* GST), which hydrogen-bonds to the sulfur atom of GSH, probably stabilizes and orientates the thiolate in a productive fashion (25). On the other hand, a kinetic analysis has been performed on this (26) and other GSTs (27), which demonstrated that the thiol proton of GSH is released during the binding of substrate. To be precise, the amount of protons released between pH 5.05 and 7.43 is stoichiometric to the amount of thiolate formed in the G-site, being the n_{H^+} of ~0.5 H^+/subunit at pH 6.5 (26).

On the other hand, since n_{H^+} is practically zero ($n_{H^+} = -0.02 \pm 0.01$) for the binding of the inhibitor *S*-hexylGSH to the wild-type hGSTP1-1, no protons are exchanged during this association. This result suggests that the protons released during the binding of substrate (GSH) to the wild-type enzyme

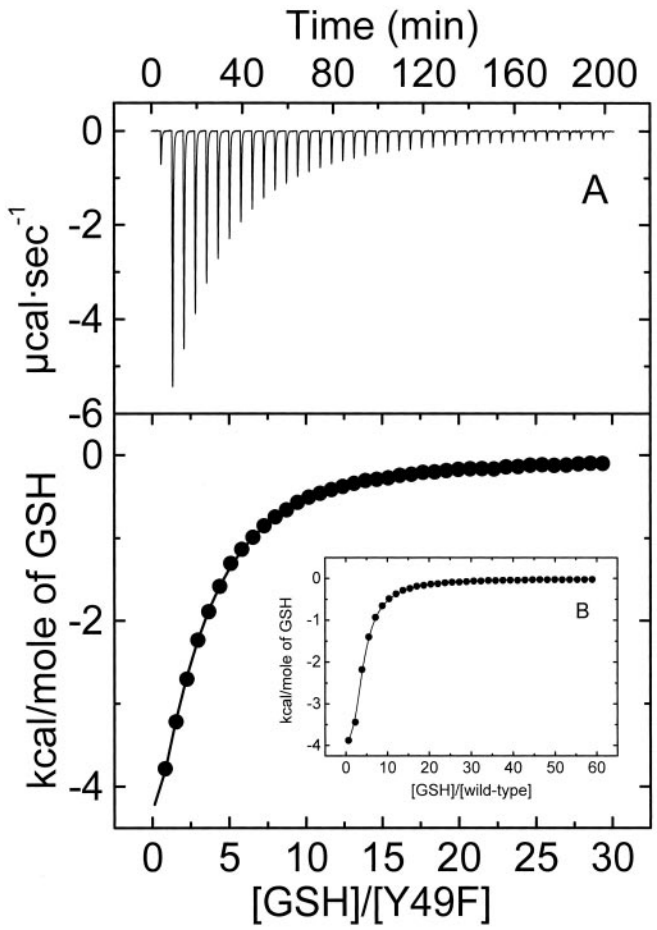

FIG. 3. *A*, representative isothermal titration calorimetry measurements of the binding of GSH to Y49F mutant of hGST P1-1. Titrations were performed in 50 mM sodium phosphate, 5 mM NaCl, 0.1 mM EDTA, and 1 mM DTT at pH 6.5 and 20 °C. A solution 46.98 μM mutant was titrated with 9.12 mM GSH. The GSH was injected into the sample cell. *B* (*inset*), integrated heats per mol of GSH injected into a solution of wild-type enzyme, in the same conditions as the mutant. 22.31 μM wild type was titrated with 9.82 mM GSH. For details, see "Experimental Procedures."

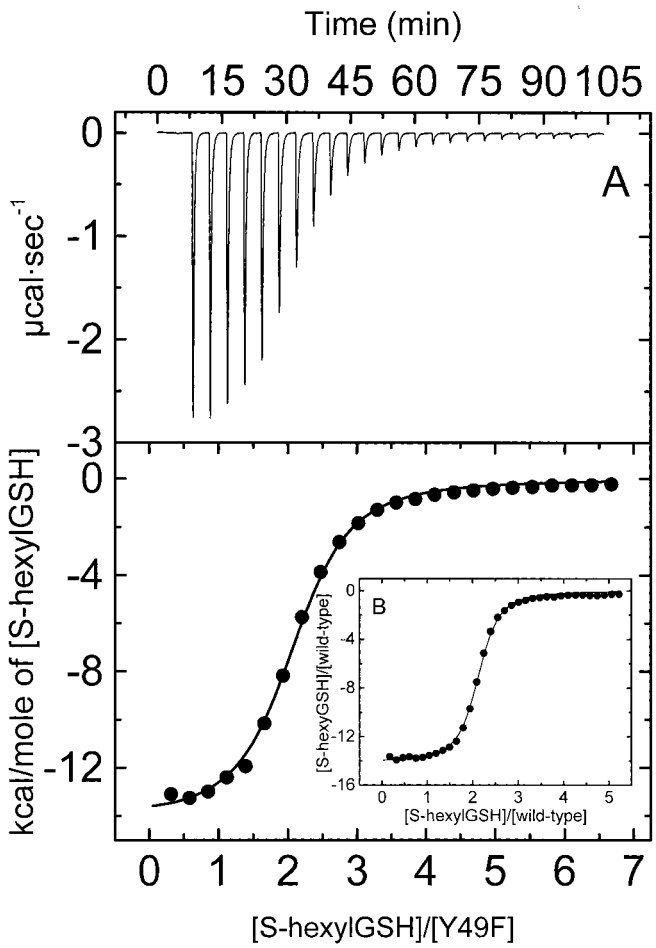

FIG. 4. *A*, representative isothermal titration calorimetry measurements of the binding of *S*-hexylGSH to Y49F mutant of hGST P1-1. Titrations were performed in 50 mM sodium phosphate, 5 mM NaCl, 0.1 mM EDTA, and 1 mM DTT at pH 6.5 and 20 °C. A 15.32 μM solution of mutant was titrated with 1.12 mM *S*-hexylGSH. The *S*-hexylGSH was injected into the sample cell. *B* (*inset*), integrated heats per mol of *S*-hexylGSH injected into a solution of wild-type enzyme, in the same conditions as the mutant. 32.66 μM wild type was titrated with 1.31 mM *S*-hexylGSH. For details, see "Experimental Procedures."

might come from the thiol group of the sulfhydryl of GSH. An analogous result was obtained by potentiometric measurements with this transferase (26) and by isothermal calorimetry for GST from *S. japonicum* (21, 28). However, in the formation of the *S*-hexylGSH-Y49F complex, there exists a net concomitant uptake of protons (n_{H^+} = 0.24 ± 0.09) (Table III). The results for the Y49F mutant can be explained by assuming that the mutation induces slight changes in the environment of the G-site, producing a shift in the pK_a of one or more groups of the ligand and/or enzyme when the complex forms. In this case, it cannot be assumed that only the sulfhydryl group of GSH is responsible for the exchange of protons at this pH, since the binding of *S*-hexylGSH to Y49F should therefore take place without exchange of protons, which is contrary to our results. Overall the following can be deduced: 1) the proton of the thiol group of GSH is released on binding to both Y49F mutant and wild-type; and 2) on binding of GSH to the mutant, at least two groups participate in the exchange of protons: the sulfhydryl group of GSH and a second group with a low pK_a capable of increasing its pK_a as a consequence of binding. This second group takes up ~0.25 protons of buffer media. Whereas an unambiguous assignment of the specific residue(s) responsible for the binding-induced uptake of protons is not possible, the side chains of Asp and Glu are likely candidates as ionizing groups at pH 6.5. Crystallographic studies show that Asp[98] of the adjacent subunit is located in the active site (3) (Fig. 1). This residue (pK_a ≅ 4.8), involved in a hydrogen-bonding network around the γ-glutamate of GSH or *S*-hexylGSH, could increase its pK as a consequence of a small local conformational change, arising from the mutation, thus explaining the number of protons taken up in the association with these ligands.

Dependence of Thermodynamic Parameters on Temperature: Heat Capacity Change—Phosphate buffer was used because it is known to have only a small enthalpy of ionization ($\Delta H_{ioniz} \approx 1$ kcal·mol^{-1}) in conjunction with only a slight pK_a change with rising temperature ($\Delta pK_a/dT = -0.0028$ K^{-1}). Therefore, only small corrections to the observed binding enthalpy ΔH_{obs} were required to take into account the possible protonation/deprotonation effects upon binding.

To determine the heat capacity change associated with the binding processes of GSH and the inhibitor *S*-hexylGSH to the Y49F mutant, a series of ITC experiments were performed at different temperatures, ranging from 15 to 38 °C. The binding of these ligands to both enzymes (Y49F and wild type) is noncooperative in the temperature range analyzed, which suggests that the interaction does not produce a conformational change that affects binding of ligand to the other site in the dimer.

Thermodynamic parameters at 25 °C calculated from the titration curves are summarized in Table IV, and the temper-

TABLE III
Protonation effect

Uncertainties correspond to the S.D. of the nonlinear least squares fit of the data points of the titration curve.

Buffer	ΔH_{ioniz}	Y49F mutant		Wild type	
		GSH $-\Delta H_{obs}$	*S*-HexylGSH $-\Delta H_{obs}$	GSH $-\Delta H_{obs}$	*S*-HexylGSH $-\Delta H_{obs}$
	kcal·mol^{-1}	*kcal·mol*$^{-1}$		*kcal·mol*$^{-1}$	
Phosphate	1.22	13.04 ± 0.31	17.14 ± 0.33	9.91 ± 0.19	16.13 ± 0.26
MES	3.72			11.27 ± 0.31	15.58 ± 0.42
MOPS	5.27	13.48 ± 0.33	16.55 ± 0.41	11.67 ± 0.23	
ACES	7.53	13.74 ± 0.40	15.41 ± 0.25	12.71 ± 0.32	16.20 ± 0.45
n_{H^+}		−0.11 ± 0.01	0.24 ± 0.09	−0.44 ± 0.08	−0.02 ± 0.01

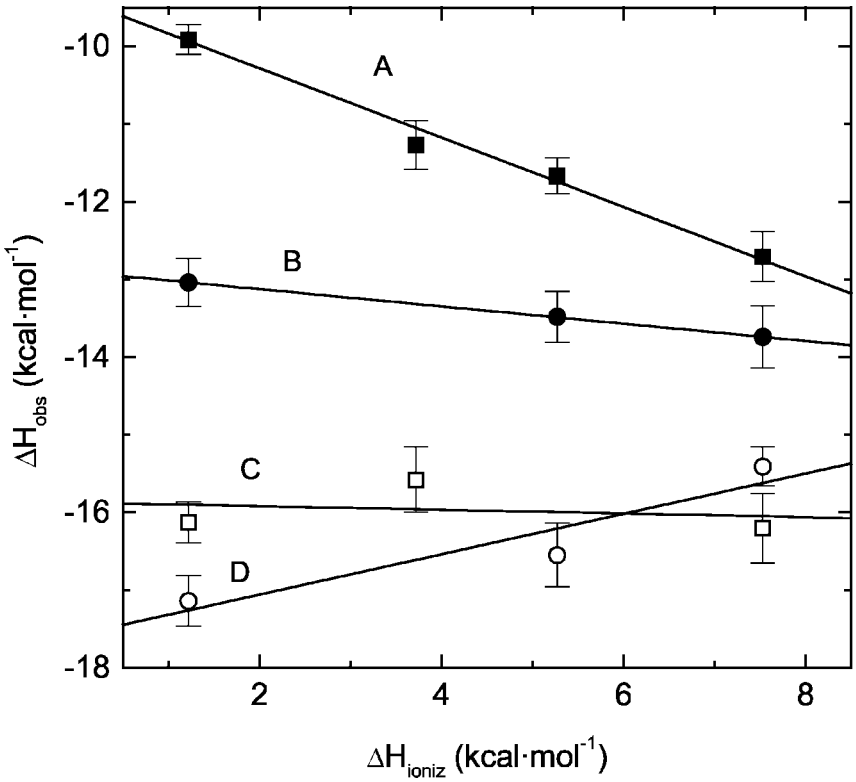

FIG. 5. **Protonation effect.** Experimentally observed enthalpy change, ΔH_{obs}, is plotted *versus* the ionization enthalpy of the buffer, ΔH_{ioniz}, at 25 °C to evaluate the protonation effect. ITC experiments were performed at pH 6.5 in phosphate, MES, ACES, and MOPS buffers. *A* and *C* correspond to titrations of the wild-type enzyme with GSH and *S*-hexylGSH, respectively. *B* and *D* correspond to titrations of Y49F mutant with GSH and *S*-hexylGSH, respectively. *Continuous lines* are linear least squares fits according to Equation 1.

ature dependence for the binding of GSH is displayed in Fig. 6. As shown in Fig. 6, ΔH and $T\Delta S^0$ strongly depend on temperature, whereas ΔG^0 is almost insensitive to the change of temperature, to both wild-type and Y49F mutant. In Fig. 6, a linear dependence of ΔH with the temperature was observed, from the slope of which the change in heat capacity (ΔC_p) upon the binding of ligand was obtained (Table IV). A plot of ΔH *versus* $T\Delta S^0$ values for the binding of GSH at different temperatures shows a slope near unity (data not shown), which is common for protein-ligand binding processes (21, 29, 30) and antibody-antigen recognition (31, 32), and has been described in terms of enthalpy/entropy compensation. This is a direct consequence of a large ΔC_p value, since $(\partial\Delta H/\partial T)_p = \Delta C_p$ and $(\partial(T\Delta S)/\partial T)_p = \Delta C_p + \Delta S$, and then if $\Delta C_p \gg \Delta S$, the changes in ΔH and $T\Delta S$ with temperature will be roughly the same ($= \Delta C_p$) and will compensate each other. ΔG^0 itself is almost unaffected over the temperature range investigated. The values of binding enthalpies and entropies over the examined temperature ranges are always negative, which is indicative that the binding process of either substrate or inhibitor to both enzymes is enthalpically favorable and entropically unfavorable.

Crystallographic Analysis of the Y49F Mutant Enzyme—The Y49F structure is essentially identical to the wild-type structure with a root mean square deviation on superposition of α-carbon atoms of 0.2 Å with no deviations greater than 0.4 Å. The aromatic ring of residue 149 superimposes almost exactly onto the ring of Tyr^{49} of the wild-type structure (Fig. 7). The mutation of Tyr^{49} to Phe causes a loss of one hydrogen bond between the hydroxyl group of Tyr^{49} and the main-chain carbonyl of Met^{91} of the opposing monomer. However, the latter moiety also takes part in other hydrogen bonding interactions, so it is no surprise that there is no change of the structure caused by the mutation.

DISCUSSION

The study presented here provides a comprehensive description of the energetics of ligand binding to the G-site of the Y49F mutant of hGST P1-1.

Fluorescence Spectroscopy

The fluorescence spectroscopy data indicate that the binding of either GSH or *S*-hexylGSH to Y49F mutant is a noncooperative process with a stoichiometry of 2 mol of ligand bound per mol of dimeric enzyme at saturation. The results obtained indicate that the Y49F mutant shows a lower affinity for binding of ligands to the G-site compared with that of wild-type enzyme. Other studies performed by equilibrium fluorescence data with hGST P1-1 show that the wild-type enzyme displays temperature-dependent cooperativity in the absence of co-sub-

TABLE IV
Thermodynamic parameters of the interaction of GSH and S-hexylGSH to Y49F mutant and the wild-type enzyme of hGST P1-1, at 25.2 °C and pH 6.5

Experimental conditions are given under "Experimental Procedures." Uncertainties correspond to the S.D. of the nonlinear least squares fit of the data points of the titration curve. K, binding constant; ΔG^0, ΔH, $T\Delta S^0$, and $\Delta C_p{}^0$, change in Gibbs energy, binding enthalpy, entropy, and heat capacity, respectively. $\Delta\Delta G^0$, $\Delta\Delta H$, $\Delta(T\Delta S^0)$, and $\Delta\Delta C_p{}^0$ are the differences in each of the values from those of wild-type hGST P1-1.

Protein	Ligand	K	ΔG^0	$\Delta\Delta G^0$	ΔH	$\Delta\Delta H$	$T\Delta S^0$	$\Delta(T\Delta S^0)$	$\Delta C_p{}^0$	$\Delta\Delta C_p{}^0$
		M^{-1}	*kcal·mol*$^{-1}$						*cal*K^{-1}·*mol*$^{-1}$	
Wild type	GSH	11,630 ± 302	−5.53 ± 0.02	0	−11.21 ± 0.12	0	−5.65 ± 0.12	0	−294.2 ± 2.7	0
Y49F	GSH	3883 ± 83	−4.88 ± 0.01	0.65 ± 0.03	−13.04 ± 0.14	−1.83 ± 0.26	−9.17 ± 0.14	−3.51 ± 0.26	−199.5 ± 26.9	95 ± 29.6
Wild type	*S*-hexylGSH	(8.1 ± 0.3)·10^5	−8.04 ± 0.02	0	−16.13 ± 0.07	0	−8.04 ± 0.07	0	−441.6 ± 48.7	0
Y49F	*S*-hexylGSH	(4.3 ± 0.1)·10^5	−7.66 ± 0.02	0.37 ± 0.04	−17.14 ± 0.08	−1.01 ± 0.15	−9.45 ± 0.08	−1.41 ± 0.15	−333.6 ± 28.8	108 ± 77.5

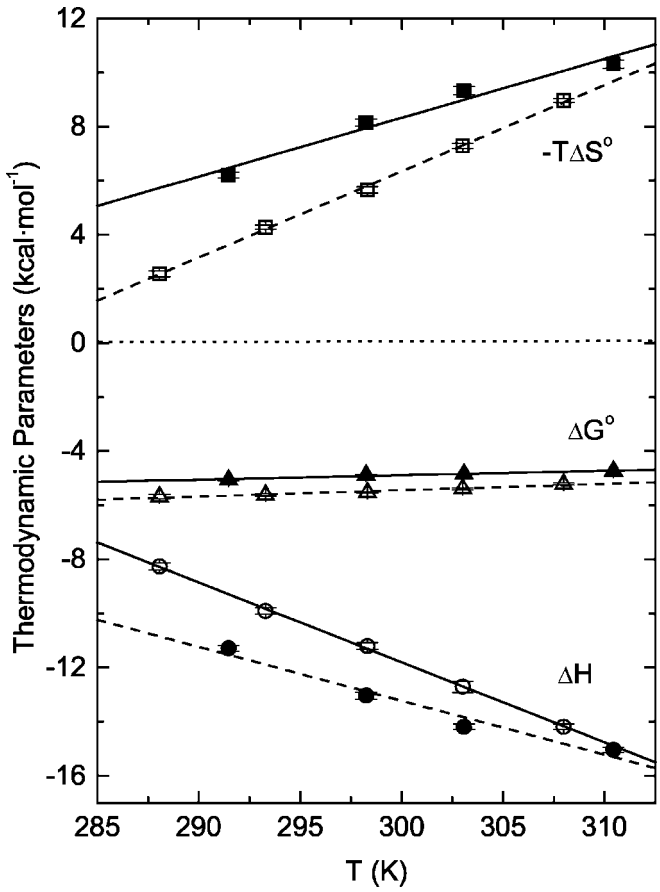

FIG. 6. **Temperature dependence of the thermodynamic parameters for binding of GSH to both the Y49F mutant and the wild-type enzyme.** The parameters for the Y49F and the wild-type enzyme are shown by *filled* and *open symbols*, respectively. The heat capacity changes, associated with the binding, were determined by linear repression analysis as the slopes of the plots of ΔH *versus* temperature and are shown in Table IV.

strate 1-chloro-2,4-dinitrobenzene (13). However, no significant cooperativity for substrate binding to GST P1-1 was detected around 25 °C (13). Furthermore, Caccuri *et al.* (13) showed that this mutant displays negative cooperativity for GSH binding at 25 °C in the presence of co-substrate 1-chloro-2,4-dinitrobenzene. However, as shown by our studies, no cooperativity was observed at this temperature in the absence of co-substrate, indicating that only in the presence of co-substrate does cooperativity exist. These results are corroborated by the ITC experiments. Thus, the replacement of Tyr^{49} by Phe results in an enzyme that retains the G-site structure and has the ability to bind ligands to the G-site of both monomers.

Calorimetric Study

Temperature Dependence of Thermodynamic Parameters—Based on thermodynamic data of the transfer of various compounds from a nonpolar phase to water (33, 34), as well as protein-folding data (35, 36) and the binding of several ligands to their cognate proteins (35, 37), it has been argued that the main contributions to a negative value of $\Delta C_p{}^0$ could be a consequence of an increase in hydrophobic interaction (35, 38), the burial of nonpolar surface area from water (38), and the presence of waters buried in the interface and/or local folding due to binding (37). In contrast, polar surfaces, when removed from the aqueous phase, increase $\Delta C_p{}^0$. The most likely explanation of this phenomenon is that hydration of a solute induces, relative to bulk water, a solvent reorganization in its first hydration shell (39, 40). The negative values of the heat capac-

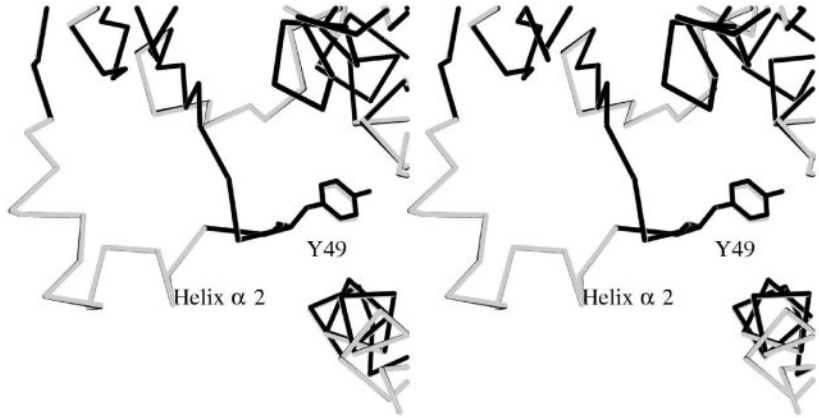

FIG. 7. **Stereoview of the region in hGST P1-1 about the site of mutation.** The α-carbon trace of the Y49F crystal structure is shown in *light gray*, and the wild-type crystal structure is shown in *black* (5GSS) (3). This *figure* was produced using MOLSCRIPT (50).

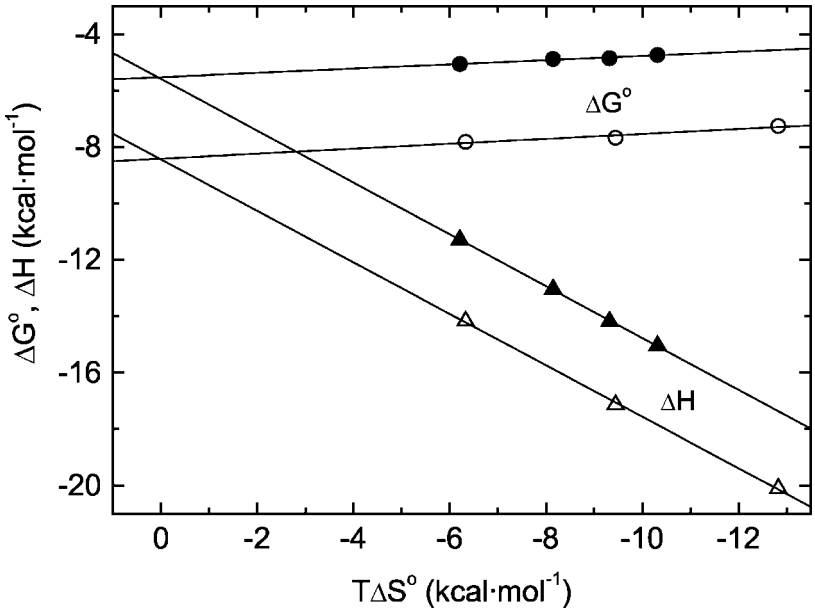

FIG. 8. **Enthalpy-entropy compensation plot for the binding of GSH (*solid symbols*) and *S*-hexylGSH (*open symbols*) to the Y49F mutant of hGST P1-1.** The dependence of ΔG^0 and ΔH *versus* $T\Delta S^0$ is shown by *circles* and *triangles*, respectively.

ity change ($\Delta C_p{}^0$), calculated for the binding of either substrate or *S*-hexylGSH to the mutant Y49F, decreased ~100 cal·K^{-1}·mol^{-1} in comparison with those for wild-type enzyme (Table IV). This increase in the values of $\Delta C_p{}^0$ may originate from releasing water molecules in the interface. This indicates that the binding of these ligands produces a higher degree of water molecule loss in the wild type than that in the Y49F mutant. The loss of water molecules is accompanied by an increase in the entropy change. This suggestion is supported by a comparison of the entropy values of both enzymes (Table IV), since the entropy changes are slightly higher for the wild-type enzyme at all temperatures (Fig. 6).

The negative $\Delta C_p{}^0$ causes the net thermodynamic driving force for association to shift from an entropic to an enthalpic contribution with increasing temperature. At the intersection point of both lines in Fig. 8, $\Delta G^0 = \Delta H$, with the entropic contribution to the binding process being zero. This intersection point corresponds to a temperature, T_S, at which the entropic contribution to the Gibbs energy of the binding changes from favorable to unfavorable. From the linear fits to the data shown in Fig. 8, the ΔH values for each T_S value, $\Delta H(T_S)$, are calculated (Table V). An enthalpic counterpart of T_S exists, namely T_H, the temperature at which the enthalpic contribution to the Gibbs energy of binding changes from unfavorable to favorable. T_H, corresponding to a zero value of ΔH, is calculated from the linear fit of Fig. 8. Therefore, at temperatures below T_H, the binding process is completely entropy-driven, whereas at temperatures above T_S, the binding process is completely enthalpy-driven. Only in the temperature interval between T_H and T_S are both of the enthalpic and the entropic parts of the Gibbs energy of binding favorable. Our results show an interval ΔT larger for the mutant than that for wild-type enzyme. However, the temperatures at which both contributions to ΔG^0 are favorable are lower for the mutant (Table V).

TABLE V
Heat capacity change, T_S, and T_H for the binding of substrate and S-hexylGSH to Y49F and wild-type enzyme of hGST P1-1

Protein	Ligand	$\Delta C_p{}^0$	$T_S{}^a$	$T_H{}^a$	$\Delta H(T_S)^b$	$\lvert\Delta T\rvert^c$
		cal·K^{-1}·mol^{-1}	*°C*	*°C*	*kcal/mol*	*°C*
Wild type	GSH	−294.20	7	−16	−6.04	9
Y49F	GSH	−199.52	−11	−38	−5.52	27
Wild type	*S*-hexylGSH	−441.63	9	−12	−8.94	3
Y49F	*S*-hexylGSH	−333.65	0	−25	−8.42	25

[a] Temperatures where entropic and enthalpic contributions to the interaction is zero.
[b] Enthalpy change where the entropic contribution to the interaction is zero.
[c] $|T_S - T_H|$.

The behavior described above is not unusual for processes characterized by a large negative ΔC_p. For example, the thermodynamics of the transfer of benzene from aqueous solution

TABLE VI
Entropy change of the interaction of GSH and S-hexylGSH with mutant Y49F of hGST P1-1 at 25.2 °C

Calculations were done according to the method of Murphy *et al*. (45), and the procedures are summarized briefly under "Experimental Procedures." $\Delta\Delta S$, $\Delta\Delta S_{solv}$, and $\Delta\Delta S_{conf}$ are the differences in each of the values from those wild-type hGST P1-1.

Protein	Ligand	ΔS_{total}[a]	$\Delta\Delta S$	ΔS_{solv}	$\Delta\Delta S_{solv}$[b]	ΔS_{conf}	$\Delta\Delta S_{conf}$
				cal·K⁻¹·mol⁻¹			
Wild type	GSH	−18.97	0	75.73	0	−86.8	0
Y49F	GSH	−27.31	−8.34	51.35	−24.38	−70.7	16.1
Wild type	*S*-hexylGSH	−26.96	0	113.66	0	−132.7	0
Y49F	*S*-hexylGSH	−31.66	−4.70	85.87	−27.80	−109.6	23.1

[a] Data from Table IV.
[b] Calculated from the equation $\Delta S_{solv} = \Delta C_p \ln(298.4/386)$.

to pure liquid (41) exhibit characteristic thermodynamic behavior similar to that shown in Figs. 6 and 8. Therefore, these thermodynamic binding characteristics are again a consequence of the negating of the hydrophobic hydration of the ligand. Note that the type of ligand does not seem to be important at this temperature interval. The superposition of the mutant Y49F structure with that for the wild-type (Protein Data Bank entries 22GS and 5GSS, respectively) shows no deviations greater than 0.4 Å. Thus, the mutation does not appear to affect the overall structure. These results can be explained only if the binding process for each ligands is similar and, consequently, also the forces responsible for the binding are similar.

Van der Waals interactions and hydrogen bonding are usually considered to be the major potential sources of negative ΔH values (35). The binding of either GSH or *S*-hexylGSH to Y49F mutant is enthalpically favorable at all temperatures studied, for which we suggest that van der Waals interactions and hydrogen bonds will be the major contribution to the energetic of binding for these ligands with the Y49F mutant. Taking into account the high similarity for both Tyr^{49} and wild-type structures, an analogous behavior could be deduced for the wild-type enzyme. In order to determine the contributions of the electrostatic interactions to this binding, we investigated the effects of ionic strength on binding of GSH to this enzyme in phosphate buffer with NaCl concentrations varying from 2 mM to 0.4 M at pH 6.5. The thermodynamic parameters obtained by ITC suggest that there is no significant effect of the ionic strength on ΔG^0, ΔH, and ΔS^0. These results suggest that electrostatic interactions are not significant in ensuring a functioning the active site region, in contrast with the Sigma/Theta GST classes (42). A similar insensitivity to ionic strength in the binding of substrate was also found in Sj26GST (43).

The data reported here indicate that the mutation leads to increased changes in both negative enthalpy and negative entropy (Table IV and Fig. 6). The negative Gibbs energy decreases as a consequence of the mutation, so the affinity of ligands (GSH and *S*-hexylGSH) for Y49F is lower than that for the wild-type enzyme. This behavior was observed at all temperatures studied (Fig. 6). Moreover, the equilibrium constant values, at all temperatures studied, are consistent with the integrated form of the van't Hoff equation. These results suggest that although the interaction between the Y49F mutant and the substrate is enthalpically more favorable than that for wild-type enzyme, the entropic loss due to binding is also increased, indicating that the mutation is both enthalpically favorable and entropically unfavorable (Table IV). A similar result was obtained for the binding of *S*-hexylGSH to wild type and the Y49F mutant. This means that the thermodynamic effect of this mutation is to decrease the entropic loss due to binding. The unfavorable entropy change outweighs the enthalpic advantage, resulting in a 3-fold lower binding constant for the binding of GSH to the wild-type enzyme. However, in the case of the interaction of S-hexylGSH with Y49F mutant, only slight increases in negative enthalpy ($\Delta\Delta H$) and negative entropy ($T\Delta\Delta S$) have been observed in comparison with those of the wild-type hGST P1-1. The binding constant of the interaction between Y49F mutant and the inhibitor *S*-hexylGSH is 2-fold lower, although the same order of magnitude as that found for the wild-type hGST P1-1. The structural studies of the complexes formed between the wild-type hGST P1-1 and some inhibitors (1, 3) have indicated that the hydroxyl group of Tyr^{49} forms a hydrogen bond with the carbonyl oxygen atom of the Met^{91} residue of the adjacent subunit (Fig. 1). In addition, 14 van der Waals contacts are also formed with the adjacent monomer (13). From these experimental data, it has been suggested that the formation of a hydrogen bond with the ligands results in a large decrease of negative entropy change due to the removal of the water molecules (44). Processes with a negative entropy change may be ascribed to hydrogen bond formation, a decrease in the number of isoenergetic conformations, or a decrease in soft internal vibrational modes (35). Processes with a positive entropy change may arise from the burial of electrostatic charges or hydrophobic groups from water (35). A greater increase in both negative enthalpy and negative entropy in the interaction with *S*-hexylGSH than those for the interaction with the substrate could be explained by the formation of a large number of hydrogen bonds in the binding with the inhibitor. However, the crystallographic studies of the complex wild type-*S*-hexylGSH shows that the same hydrogen bonds occur as those in the complex with GSH (3). It is known, however, that an increase in the apolarity of a medium increases the strength of the hydrogen bonds, and consequently, the negative contribution to enthalpy and entropy changes will be higher. Thus, the increase in the negative values in both entropy and enthalpy of the binding with *S*-hexylGSH, with respect to GSH, may be a consequence of a higher apolarity in the environment of the active site, provided by the hexyl chain of the inhibitor. This also could explain the higher affinity of the inhibitor than that of the substrate.

TABLE VII
Entropic contributions of the interaction of Y49F mutant of hGST P1-1 with GSH and S-hexylGSH and the number of residues, $\mathcal{R}$, participating in the binding

Protein	Ligand	T_S	$\Delta S_{HE}(T_S)$[a]	ΔS_{others}	$\mathcal{R}$
		°C	*cal·K⁻¹·mol⁻¹*	*cal·K⁻¹·mol⁻¹*	
Wild type	GSH	7	127.3	−177.3	31.7
Y49F	GSH	−11	104.2	−154.2	27.5
Wild type	*S*-hexylGSH	9	186.7	−236.7	42.3
Y49F	*S*-hexylGSH	0	155.7	−205.7	36.7

[a] Calculated from the equation $\Delta S_{HE}(T_S) = 1.35\Delta C_p \ln(T_S/386)$.

Entropic Contribution Responsible for the Different Affinities—According to the considerations of Murphy *et al.* (45), the total ΔS of binding is given as follows,

$$\Delta S = \Delta S_{solv} + \Delta S_{conf} + \Delta S_{crat} \quad \text{(Eq. 2)}$$

where ΔS_{solv} is the change in entropy derived from solvent release upon binding, ΔS_{conf} is the change in entropy resulting from conformational changes due to formation of complex, and ΔS_{crat} is the cratic entropy change. ΔS_{solv} is given by $\Delta S_{solv} = \Delta C_p \ln(T/T_S)$ (T_S = 386 K; T_S is the temperature at which the solvation entropy change is considered to be zero), and ΔS_{crat} can be considered a constant value (-7.9 cal·mol^{-1}·K^{-1}) (33, 46). From the experimental data, it can be suggested that the desolvation entropy loss is, to a large extent, compensated by the conformational entropy. As can be observed from Table VI, the binding of ligands to the mutant produces a loss of entropy (negative $\Delta\Delta S_{solv}$) with respect to the same interaction with the wild-type enzyme. Thus, the extra unfavorable ΔS_{solv} (negative value) for both ligands (substrate and inhibitor) will be the entropic component responsible for the decrease in the affinity of the mutant enzyme.

Residue Numbers Involved in the Association—Recently, Spolar and Record (37) proposed that local folding can be coupled to ligand binding. According to their proposal, total entropy change can be described as $\Delta S = \Delta S_{HE} + \Delta S_{RT} + \Delta S_{others}$, where ΔS_{HE} is the entropy change from hydrophobic interactions, which is related to the heat capacity change, and ΔS_{RT} originates from rotational and translational change and is considered to be constant (50 cal·mol^{-1}·K^{-1}) (37). At the temperature T_S, $\Delta S = 0$ and then $\Delta S_{HE}(TS) + \Delta S_{RT} + \Delta S_{others} = 0$. If the entropy change due to a small conformational change is considered to be equal for each residue, the entropy change is calculated to be 5.6 cal·K^{-1}·mol^{-1}, and thus division of ΔS_{others} by -5.6 yields the number of residues involved in the conformational change: $\Re = \Delta S_{others}/-5.6$. We have used this description to estimate the number of the residues, $\Re$, involved in the binding processes characterized in our study (Table VII). In the binding of *S*-hexylGSH to the wild-type enzyme, the $\Re$ value was increased to 9, with respect to that for the binding of GSH. An identical increment was obtained for the binding of these ligands to Y49F. This result can be expected from the comparison of the structures of both ligands bound to wild-type. In the case of the *S*-hexylGSH, the aliphatic moiety occupies the H-site (3), and the number of interactions with residues of the G-site increases with respect to the interactions of substrate. On the other hand, for the same ligand, the number of residues involved in the binding decreases in the mutant enzyme with respect to the wild type. This can be explained, assuming that the substitution of tyrosine 49 by phenylalanine produces a local conformational change in the vicinity of the active site. Thus, on the basis of this description, small alterations produced by the mutation are deduced to occur in the active site. Large conformational changes or structural changes induced by the ligand binding are not predicted from the thermodynamic parameters obtained in this study.

Changes on Solvent-accessible Surface Areas—Finally, the observed values of ΔC_p^0 can be used to estimate the amount of both polar and apolar surfaces buried on binding. Relationships documented in the literature (47, 48) have been used to calculate the amount of polar and apolar interfacial surface necessary to account for the observed ΔC_p^0 values. Note that these relationships are intended to relate ΔC_p^0 for protein folding transitions to the loss of solvent-accessible surface and, thus, may, or may not be adequate to apply to all protein-ligand interactions. Changes in apolar (ΔASA_{ap}) and polar (ΔASA_p) solvent-accessible surface areas upon complexation have been estimated by those relationships mentioned above. On the basis of the x-ray crystallographic data of several proteins, the changes in the water-accessible surface areas of both nonpolar (ΔASA_{ap}) and polar (ΔASA_p) residues on protein folding have been calculated. Such calculations reveal that the ratio $\Delta ASA_{ap}/\Delta ASA_p$ varies between 1.2 and 1.7 (47). This range is comparable with the medium value for the ratio of $\Delta ASA_{ap}/\Delta ASA_p$ of ~1.2, calculated for the interactions described in this study. The application of Murphy's approach (47) to the experimentally determined values indicates that the surface areas buried on complex formation comprise ~54% of the nonpolar surface. Therefore, as Spolar and Record (37) indicate, these values can be taken as the "rigid body" interactions, and therefore, no large conformational changes can occur as a consequence of the association with these ligands.

Acknowledgment—We thank Dr. Lorenzo Stella very much for helpful advice about the fluorescence spectra measurements.

REFERENCES

1. Reinemer, P., Dirr, H. W., Ladenstein, R., Huber, R., Lo Bello, M., Federici, G., and Parker, M. W. (1992) *J. Mol. Biol.* **227,** 214–222
2. Lo Bello, M., Oakley, A. J., Battistoni, A., Mazzetti, A. P., Nuccetelli, M., Mazzarese, G., Rossjohn, J., Parker, M. W., and Ricci, G. (1997) *Biochemistry* **36,** 6207–6217
3. Oakley, A. J., Lo Bello, M., Battistoni, A., Ricci, G., Rossjohn, J., Villar, H. O., and Parker, M. W. (1997) *J. Mol. Biol.* **274,** 84–100
4. Mannervik, B., Alin, P., Guthenberg, C., Jensson, H., Tahir, M. K., Warholm, M., and Jörnvall, H. (1985) *Proc. Natl. Acad. Sci. U. S. A.* **82,** 7202–7206
5. Meyer, D. J., Coles, B., Pemble, S. E., Gilmore, K. S., Fraser, G. M., and Ketterer, B. (1991) *Biochem. J.* **274,** 409–414
6. Pemble, S. E., Wardle, A. F., and Taylor, J. B. (1996) *Biochem. J.* **319** 749–754
7. Meyer, D. J., and Thomas, M. (1995) *Biochem. J.* **311** 739–742
8. Board, P. G., Baker, R. T., Chelvanayagam, G., and Jermiin, L. S. (1997) *Biochem. J.* **328,** 929–935
9. Armstrong, R. N. (1997) *Chem. Res. Toxicol.* **10,** 2–18
10. Caccuri, A. M., Ascenzi, P., Antoninio, G., Parker, M. W., Oakley, A. J., Chiessi, E., Nuccetelli, M., Battistoni, A., Bellizia, A., and Ricci, G. (1996) *J. Biol. Chem.* **271,** 16193–16198
11. Ricci, G., Caccuri, A. M., Lo Bello, M., Rosato, N., Mei, G., Nicotra, M., Chiessi, E., Mazzetti, A. P., and Federici, G. (1996) *J. Biol. Chem.* **271,** 16187–16192
12. Oakley, A. J., Lo Bello, M., Ricci, G., Federici, G., and Parker, M. W. (1998) *Biochemistry* **37,** 9912–9917
13. Caccuri, A. M., Antonini, G., Ascenzi, P., Nicotra, M., Nuccetelli, M. Mazzetti, A. P., Federici, G., Lo Bello, M., and Ricci, G. (1999) *J. Biol. Chem.* **274,** 19276–19280
14. Lo Bello, M., Battistoni, A., Mazzetti, A. P., Board, P. G., Muramatsu, M., Federici, G., and Ricci, G., (1995) *J. Biol. Chem.* **270,** 1249–1253
15. Picard, V., Ersdal-Badju, E., Lu, A., and Bock, S. C., (1994) *Nucleic Acids Res.* **22,** 2587–2591
16. Gill, S. C., and von Hippel P. H. (1989) *Anal. Biochem.* **182,** 319–326
17. Otwinowski, Z. (1993) in *Data Collection and Processing* (Sawyer, L. Isaacs, N., and Bailey, S., eds) pp. 56–62, SERC Daresbury Laboratory, Warrington, UK
18. CCP4 (1994) *Acta Crystallogr. Sect. D* **50,** 750–763
19. Brünger, A. T., (1993) *X-PLOR: A System for X-ray Crystallography and NMR*, Version 3.1, Yale University Press, New Haven, CT
20. Laskowski, R. A., MacArthur, M. W., Moss, D. S., and Thornton, J. M. (1993) *J. Appl. Crystallogr.* **26,** 283–291
21. Ortiz-Salmerón, E., Yassin, Z., Clemente-Jiménez, M. J., Las Heras-Vazquez, F. J., Rodríguez-Vico, F., Barón, C., and García-Fuentes, L. (2001) *Eur. J. Biochem.* **268,** 4307–4314
22. Wiseman, T., Williston S., Brandts J. F., and Lin L. N. (1989) *Anal. Biochem.* **17,** 131–137
23. Fukada, H., and Takahashi, K. (1998) *Proteins* **33,** 159–166
24. Cooper, A., and Johnson, C. M. (1994) *Methods Mol. Biol.* **22,** 109–124
25. Armstrong, R. N. (1991) *Chem. Res. Toxicol.* **4,** 131–139
26. Caccuri, A. M., Lo Bello, M., Nucetelli, M., Nicotra, M., Rossi, P., Antonini, G., Federici, G., and Ricci, G. (1998) *Biochemistry* **37,** 3028–3034
27. Caccuri, A. M., Antonini, G., Board, P. G., Parker, M. W., Nicotra, M., Lo Bello, M., Federici, G., and Ricci, G. (1999) *Biochem. J.* **344,** 419–425
28. Ortiz-Salmerón, E., Yassin, Z., Clemente-Jiménez, M. J., Las Heras-Vazquez, F. J., Rodríguez-Vico, F., Barón, C., and García-Fuentes, L. (2001) *Biochim. Biophys. Acta* **1548,** 106–113
29. Dam, T. K., Oscarson, S., and Brewer, C. F. (1998) *J. Biol. Chem.* **273,** 32812–32817
30. García-Fuentes, L., Cámara-Artigas, A., López-Mayorga, O., and Barón C. (1996) *J. Biol. Chem.* **271,** 27569–27574
31. Hibbits, K. A., Gill, D. S., and Wilson, R. C. (1994) *Biochemistry* (*Mosc.*) **33,** 3584–3590
32. Swaminathan, C. P., Nandi, A., Visweswariah, S. S., and Surolia, A. (1999) *J. Biol. Chem.* **274,** 31272–31278
33. Murphy, K. P., Privalov., P. L., and Gill, S. J. (1990) *Science* **247,** 559–561
34. Spolar, R. S., Livingstone, J. R., and Record, M. T. (1992) *Biochemistry* **31,** 3947–3955
35. Sturtevant, J. M. (1977) *Proc. Natl. Acad. Sci. U. S. A.* **74,** 2236–2240
36. Spolar, R. S. Ha, J. H., and Record, M. T. (1989) *Proc. Natl. Acad. Sci. U. S. A.* **86,** 8382–8385
37. Spolar, R. S., and Record, M. T. (1994) *Science* **263,** 777–784
38. Stites, W. E. (1997) *Chem. Rev.* **97,** 1233–1250

39. Sharp, K. A., and Madan, B. (1997) *J. Phys. Chem. B* **101,** 4343–4348
40. Lee, B. (1994) *Biophys. Chem.* **51,** 271–278
41. Ha, J. H., Spolar, R. S., and Record, M. T. (1989) *J. Mol. Biol.* **209,** 801–816
42. Stevens, J. M., Armstrong R. N., and Dirr, H. (2000) *Biochem. J.* **347** 193–197
43. Yassin, Z., Clemente-Jiménez, M. J., Téllez-Sanz, R., and García-Fuentes, L. (2003) *Int. J. Biol. Macromol.* **31,** 155–162
44. Connelly, P. R., Aldape, R. A., Bruzzese, F. J., Chambers, S. P., Fitzgibbon, M. J., Fleming, M. A., Itoh, S., Livingston, D. J., Navia, M. A., and Thomson, J. A. (1994) *Proc. Natl. Acad. Sci. U. S. A.* **91,** 281–293
45. Murphy, K. P., Freire, E., and Paterson, Y. (1995) *Proteins Struct. Funct. Genet.* **21,** 83–90
46. Baldwin, R. L. (1986) *Proc. Natl. Acad. Sci. U. S. A.* **83,** 8069–8072
47. Murphy, K. P., and Freire, E. (1992) *Adv. Protein Chem.* **3,** 313–361
48. Hilser, V. J., Gómez, J., and Freire, E. (1996) *Proteins* **26,** 123–133
49. Humphrey, W., Dalke, A., and Schulten, K. (1996) *J. Mol. Graphics* **14,** 33–38
50. Kraulis, P. J. (1991) *J. Appl. Crystallogr.* **24,** 946–950

Thermodynamic Description of the Effect of the Mutation Y49F on Human Glutathione Transferase P1-1 in Binding with Glutathione and the Inhibitor *S*-Hexylglutathione

Emilia Ortiz-Salmerón, Marzia Nuccetelli, Aaron J. Oakley, Michael W. Parker, Mario Lo Bello and Luis García-Fuentes

J. Biol. Chem. 2003, 278:46938-46948.
doi: 10.1074/jbc.M305043200 originally published online August 23, 2003
